Steering light with magnetic textures

Ioan-Augustin Chioar, Christina Vantaraki, Merlin Pohlit, et al.

View Online   Export Citation   CrossMark

ARTICLES YOU MAY BE INTERESTED IN

Steering light with magnetic textures

View Online　Export Citation　CrossMark

Ioan-Augustin Chioar,[1,a)] (iD) Christina Vantaraki,[1] Merlin Pohlit,[1] Richard M. Rowan-Robinson,[1,b)] (iD)
Evangelos Th. Papaioannou,[2] (iD) Björgvin Hjörvarsson,[1] (iD) and Vassilios Kapaklis[1,c)] (iD)

AFFILIATIONS

[1]Department of Physics and Astronomy, Uppsala University, Box 516, SE-75120 Uppsala, Sweden
[2]Institut für Physik, Martin-Luther-Universität Halle-Wittenberg, Von-Danckelmann-Platz 2, 06120 Halle, Germany

[a)]Current address: Department of Applied Physics, Yale University, New Haven CT 06511, USA.
[b)]Current address: Department of Material Science and Engineering, University of Sheffield, Sheffield, United Kingdom.
[c)]Author to whom correspondence should be addressed: vassilios.kapaklis@physics.uu.se

ABSTRACT

We study the steering of visible light using a combination of magneto-optical effects and the reconfigurability of magnetic domains in yttrium-iron garnet films. The spontaneously formed stripe domains are used as a field-controlled optical grating, allowing for active spatio-temporal control of light. We discuss the basic ideas behind the approach and provide a quantitative description of the field dependence of the obtained light patterns. Finally, we calculate and experimentally verify the efficiency of our magneto-optical grating.

Optical components are used for focusing, filtering, steering, and manipulating the polarization of light. Their properties are typically obtained by fabrication of three dimensional objects, having specific refractive indices, dichroism, or birefringence effects.[1] However, the mechanical assembly of reconfigurable components forming an optical device can limit its long-term stability and reliability. Flat optics has, therefore, been pursued in an attempt to remedy these shortcomings. The effort has given rise to a revolution in the field of optics, building upon developments in the fields of plasmonics, metamaterials, and nanofabrication.[2–5] Metamaterials facilitate the shaping of optical wavefronts[1,6,7] through the structuring of near-fields in a designer manner, thereby offering control of the far-field response.[8] These can also be reconfigured using electric and magnetic fields, temperature, mechanical agents as well as chemical reactions.[9] Magnetically controlled metamaterials are of special relevance in this context due to their reconfigurability, flexibility in design, and the fast response of opto-magnetic effects.[10,11] Therefore, investigating ways in which tailored magnetic textures can be harnessed for the design of useful optical responses is of particular interest.[11–15] In fact, related approaches for magnetic holography recording and the subsequent steering of light were initiated in the 1970s using garnet materials,[16–23] MnBi alloys,[24–26] and EuO.[27]

In light of the metamaterial approach and opportunities, we here revisit the use of yttrium-iron garnet (YIG)[16,18,22] for obtaining one of the most basic functions of an optical component: deflection of light.

The steering is obtained by applying an external magnetic field, influencing the spontaneously formed stripe-like magnetic domains, which, in turn, affect the intensity of the angular distribution of the transmitted light. We describe the connection between the magnetic texture of the YIG film and the deflected light, establishing a description of the relation between the real space magnetic domain structure and the reciprocal space, as seen from the scattered light patterns.[28–31] We also quantify the efficiency of the YIG-based grating. The ideas and results discussed here can be utilized for the design and development of a new generation of flat, reconfigurable, and potentially fast optics[10] through the control of magnetic order and textures at the mesoscale[12] using thin film technology and nanolithography.[32–37]

The investigated YIG film (30 mm × 3 mm × 7.3 μm) was grown by liquid phase epitaxy on a 500 μm thick gallium gadolinium garnet (GGG) substrate.[38,39] The angular dependence of the transmitted intensity was determined using a specially designed magneto-optical diffractometer based on a $\theta - 2\theta$ goniometer (Huber 424 2-circle goniometer). The sample was mounted in the center of a quadrupole magnet, providing vectorial magnetic fields up to 42 mT. The sample was illuminated using a supercontinuum laser (Fianium SC-400-2) with a wavelength range of 400–1100 nm or a monochromatic laser (Coherent OBIS) with a wavelength of 530 nm and a power of 20 mW. Two Glan–Thompson polarizers (Thorlabs GTH10M) were used for setting the polarization of the incoming beam and for analyzing the rotation in the detected light. The signal was modulated

to allow lock-in detection (SR830) and recorded using a Si photodiode detector (Thorlabs DET100A). A beam splitter was employed for monitoring the intensity of the source, providing on-the-fly normalization of the intensity of the incoming light. For the field dependence measurements, the sample was first saturated, ensuring a reset of the magnetic domain configuration, and thereafter brought to the targeted field before performing a detector scan. Hysteresis curves were measured for both in- and out-of-plane applied magnetic fields using a magneto-optical Kerr effect (MOKE) magnetometer. Finally, a Kerr microscope was used for magnetic imaging. To image the remanent magnetization state, the samples were first demagnetized in a time-dependent magnetic field of decaying amplitude. The microscopic data presented here are polar-MOKE (P-MOKE) contrast images in reflection.

Magnetic stripe domains are formed in the YIG film as shown in Fig. 1, constituting a one-dimensional grating-like structure for the out-of-plane magnetization component. The stripe domains can be
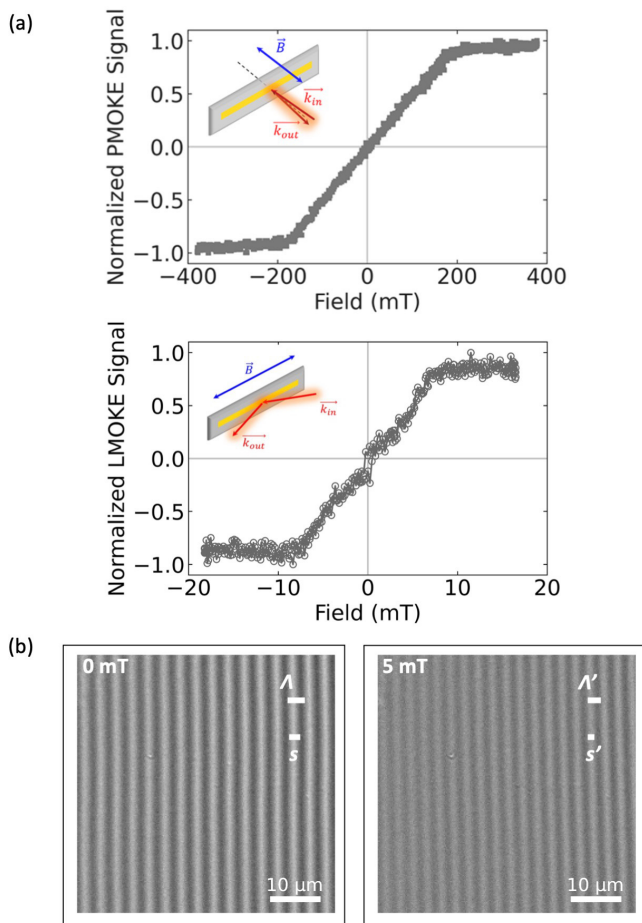
oriented[40] along any direction within the sample plane, using external in-plane magnetic fields (see also supplementary material videos). The direction of the applied in-plane magnetic field also affects the magnetic texture by primarily altering the grating periodicity (Λ) [Fig. 1(b)] with the primary domain width (s) selectively affected, depending on the in-plane field direction and magnitude.[11] For the remainder of this Letter, we will concentrate on the case where in-plane magnetic fields are applied to the YIG film along the y-direction as defined in Fig. 2.

The layout of the magneto-optical scattering experimental setup is illustrated in Fig. 2. The Faraday effect acting upon the light (polarized along the y-direction) transmitted through the YIG film results in a rotation of the polarization. Having domains of opposite out-of-plane magnetization components yields rotations of opposite signs. The interference between the light with opposite rotation of the polarization gives rise to a diffraction pattern, closely resembling that of a conventional optical grating. However, the interference arises from the phase difference of the partial waves and not a modulation in the transmitted intensity along the grating direction. Assuming a linear-response regime, we can further calculate the intensity of the transmitted diffracted beam though the YIG film. Defining F as the Faraday rotation and d as the film thickness, the rotation will be $\varphi = Fd$. Domains of opposite magnetization rotate the polarization in opposite directions ($\varphi_1 = +Fd$ for M^+ and $\varphi_2 = -Fd$ for M^-), resulting in a periodic modulation of the electric field components. Consequently, a maximum achievable efficiency in terms of change in the beam power can be estimated, knowing the attenuation coefficient a and by using (see the supplementary material for full derivation)[41]

$$\eta_{max} = \frac{4}{\pi^2} e^{-2} \left(\frac{2F}{a}\right)^2 \sin^2 \frac{\pi s}{\Lambda}. \quad (1)$$

For the YIG film used here: $F = 2200 \, \text{deg/cm}$ (experimentally determined, see the supplementary material) and $a = 1417 \, \text{cm}^{-1}$ (measured absorption coefficient, see the supplementary material), resulting in $\eta_{max} = 1.6 \times 10^{-4}$ for a wavelength of $\lambda = 530 \, \text{nm}$. This value is

FIG. 1. The magneto-optical grating. (a) Hysteresis loops of the YIG sample for out-of-plane (upper panel) and in-plane (lower panel) applied magnetic fields. (b) An in-plane magnetic field couples to the in-plane component of the magnetization in the YIG film, altering the periodicity Λ while maintaining the ratio $f = s/\Lambda = s'/\Lambda'$ between the domains. The full micromagnetic characterization of the YIG film using magnetic microscopy is detailed in the supplementary material videos.
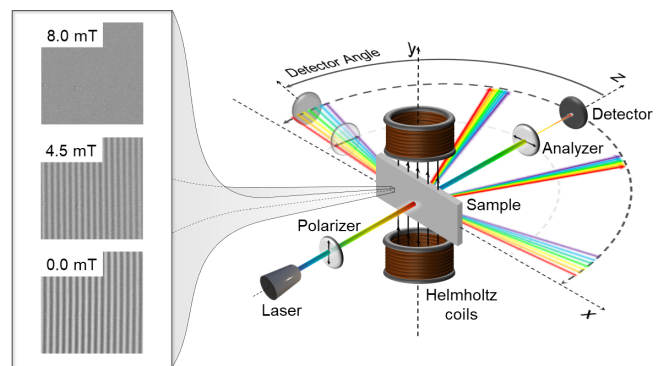

FIG. 2. Schematic description of the magneto-optical scattering setup and the field dependence of the binary magnetic YIG grating. The YIG film is illuminated using a supercontinuum laser beam at normal incidence (450–900 nm), while placed between two Helmholtz coils, providing a field along the y-direction. The laser beam is linearly polarized before reaching the sample. An analyzer is positioned in front of the detector, which can be moved in the zx plane, as depicted on the right side.

comparable to, yet higher than certain reported results in the literature, for example, MnBi magnetic gratings,[24–26,42] yet smaller than the values reported for Bi-substituted garnet materials.[17–19] It is worth noting that these improvements can imply additional chemical synthesis complexity and an intricate interplay between the magnetic properties and film thickness, which impact the angular deflection window and magneto-optical efficiency.[17,18] The actual experimental value of the efficiency for our YIG film was determined to be $\eta_{exp} = 1.47(6) \times 10^{-4}$ in reasonable agreement with the calculated value.
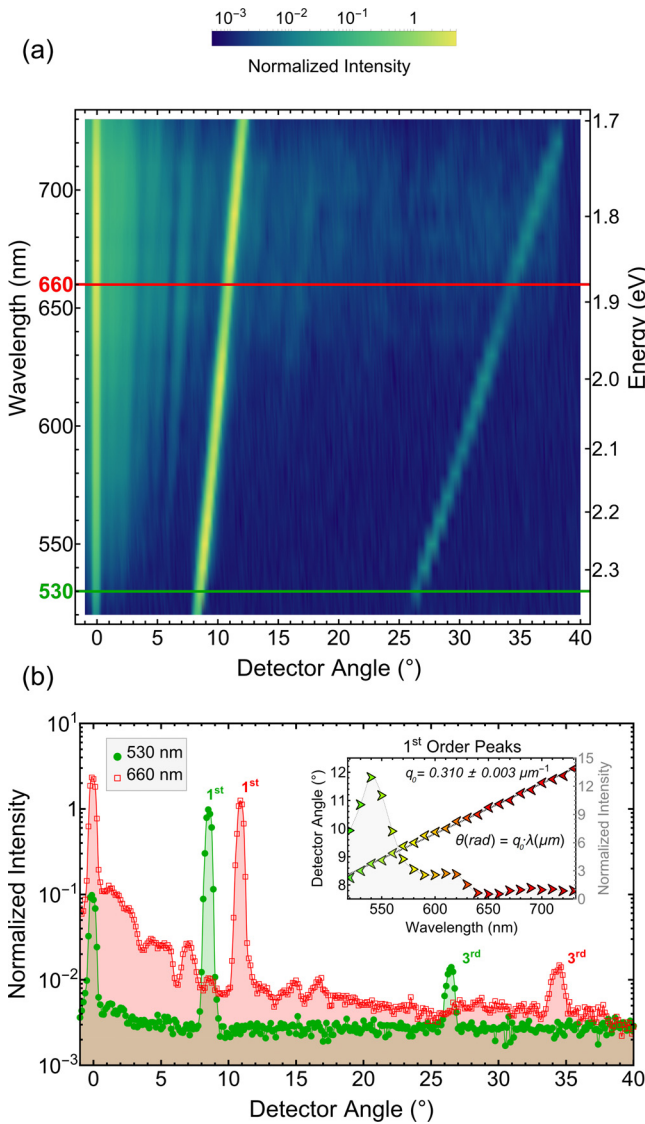
Figure 3(a) displays the wavelength and angular dependence of the transmitted light, and in Fig. 3(b), we show the angular dependence of the intensity at two wavelengths (660 and 530 nm) along with the position and the intensity of the first diffraction peak. We note the close to perfect scaling of the angular position of the peak and the wavelength of the incoming light as well as the strong wavelength dependence of the intensity of the diffracted light, reminiscent of the YIG intrinsic magneto-optical activity (see the supplementary material). The in-plane field dependence of the diffracted light is illustrated in Fig. 4. As the applied field is increased, the grating periodicity decreases, leading to an increase in the diffraction angle for any given order, while a decrease in the intensity is also recorded. The latter can be traced to Fig. 1(b), originating from a reduction in the P-MOKE contrast as the field increases.

The stripe domains disappear, as does the diffraction, when the sample is saturated. Starting from remanence and with the field applied parallel to the sample surface, a linear dependence of the angular position of the first order diffracted beam with the applied field strength is observed, almost the whole way up to magnetic saturation, as shown in the inset of Fig. 4. At the same time, the intensity of the diffracted beam is generally decreasing with the increase in the applied field, ultimately reaching zero at magnetic saturation. The decrease in the diffracted intensity originates from a reduction in the out-of-plane magnetization, thus decreasing the difference in the rotation of the polarization angle in the stripe domains. Note that the azimuthal rotation of the in-plane applied field starting from saturation results in the rotation of the scattering plane, since the stripe domains form parallel to the new field direction (see the supplementary material video).

Finally, we describe the temporal response of the YIG magneto-optical diffraction. For this purpose, we used the experimental protocol illustrated in Fig. 5(a). The time-dependent response depends on the field protocol as well as the position of the detector. Having chosen a detector angle within the angular position window of the first order peaks, we applied a sine-wave magnetic field on top of a field offset, effectively driving the sample between its saturated and remanent states. This results in a time dependency, as exemplified in the left
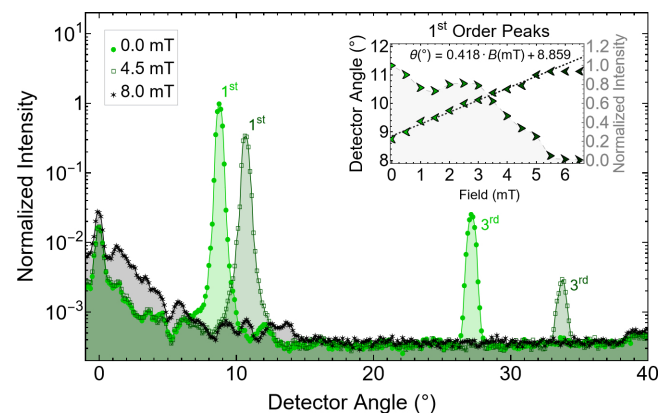

FIG. 3. Wavelength dependence of the magneto-optical scattering and the remanent magnetic state, where $\Lambda \approx 3.2~\mu m$. (a) The diffraction peaks move when the laser wavelength is changed as in the conventional optical grating. (b) Fitting the angular position of the first order peak against the laser wavelength yields the reciprocal lattice unit value $q_0 = q/(2\pi) = 1/\Lambda$ (see the supplementary material for details) shown in the inset, which closely follows the observed periodicity as observed by magneto-optical microscopy (Fig. 1).

FIG. 4. Field dependence of the magneto-optical scattering for in-plane applied fields along the y-direction (Fig. 2). All patterns were recorded using a wavelength of 530 nm. The inset shows the field dependence of the position and the intensity of the first diffraction peak. The intensities have been normalized to the first diffraction order in the absence of an applied magnetic field (0 mT).
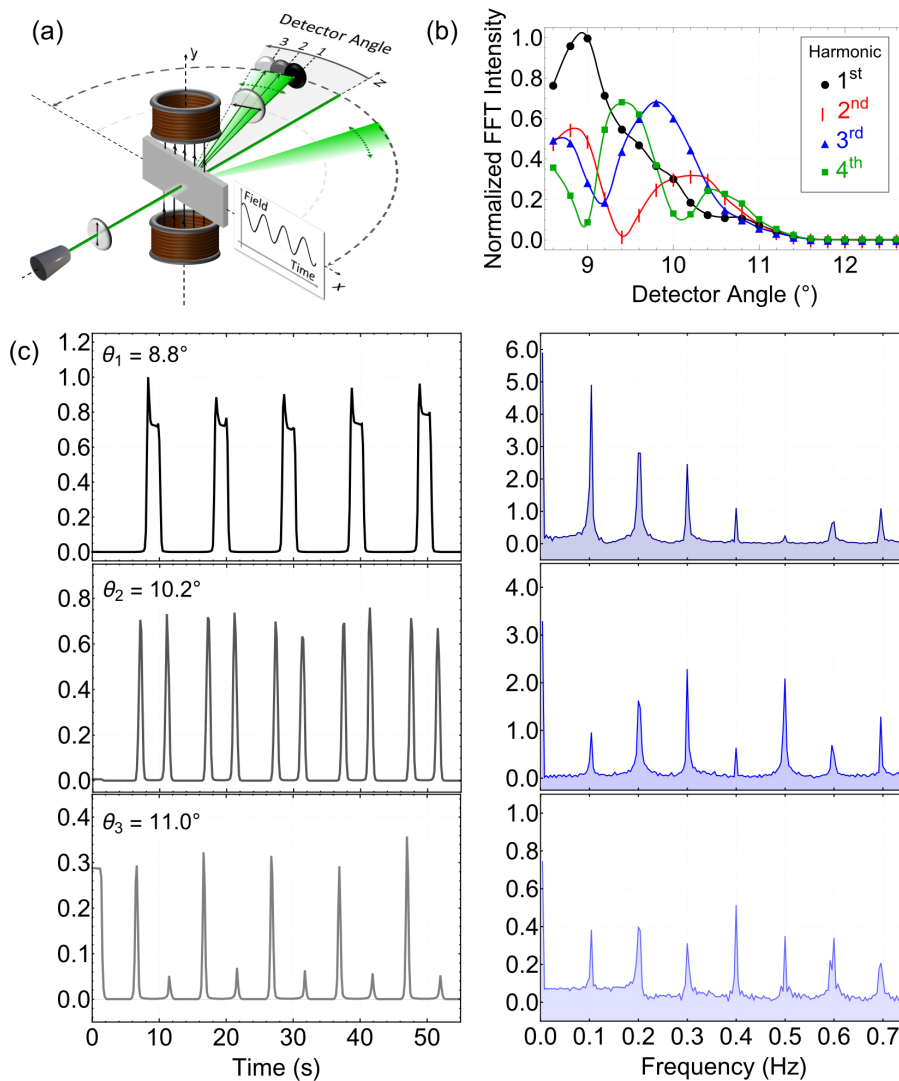
FIG. 5. Frequency modulation using magneto-optical gratings. (a) Combining the detector angular placement with a field oscillation at a given amplitude and frequency, it is possible to alter the spectral intensity content of the signal as shown in (b) by changing the beam sweeping sequence over the detector (c). In all cases shown here, an oscillating field of 5 mT amplitude, 5 mT offset, and 0.1 Hz frequency was used with the laser wavelength set to 530 nm. The recorded intensities are for the first diffraction order and detector angles of $\theta_1 = 8.8°$, $\theta_2 = 10.2°$, and $\theta_3 = 11.0°$. The intensities have been normalized to the highest intensity of the first harmonic (0.1 Hz). This highlights the tunable harmonic content, enabling modulation on frequencies above the field driving frequency.

column of Fig. 5(c). Here, we notice the large difference in response, solely arising from the choice of the detector angle. In fact, the relative positioning of the detector within the first order peak window produces signals with mixed spectral load and possibilities for beam modulation options involving tunable weighing of the harmonic content. Changing the amplitude and the sign of the applied field, i.e., performing partial or extended loops, is expected to add another degree of freedom, allowing further tailoring of the spatiotemporal steering of light. An interesting outlook also resides in the use of driving frequencies beyond the current quasi-static framework.

The concepts discussed here can be used when designing magnetically controlled flat optical devices. A foreseeable major potential for improvement lies in the field of magnetic metamaterials,[10,34,37] where the necessary magnetic domain structures can be designed and engineered utilizing lithography. For reasonably large diffraction angles to be achieved, the width of the domains must be comparable or larger than the wavelength of the light, for which nanopatterned magnetic metamaterials offer an ideal setting.[12] This can be done in combination with conventional magnetic materials rather than targeting specific magnetic materials with the required, intrinsic domain structures such as the YIG presented here. Additionally, a variety of magnetic materials suitable for fabrication of such metamaterials exhibit all-optical switching properties, where ultra-fast laser pulses may be used to set the magnetic state in nanoarrays[43,44] or films of these materials.[45–47] In this way, light cannot only be acted upon by metamaterial architectures but also be used to set this action by writing-in the necessary mesoscopic magnetic structure. Advanced design and control of such metamaterials will allow for more intricate schemes of light control,[47,48] not only in terms of the scattering but also over properties of light such as angular and orbital momenta,[49–52] holding strong promises for information technology related applications.

See the supplementary material for a detailed derivation of the magneto-optical grating equations and efficiency along with

experimental data on the photon energy-dependent Faraday rotation and absorption coefficient. We further present details on the calculation of the scattering patterns for real-space magnetic microscopy data. Two videos are included, presenting the field dependence of the magnetic domain structure alongside the resulting reciprocal space patterns and the experimentally observed light beam deflections while applying magnetic fields.

AUTHOR DECLARATIONS
Conflict of Interest

The authors have no conflicts to disclose.

DATA AVAILABILITY

The data that support the findings of this study are available from the corresponding author upon reasonable request.

REFERENCES

[1]W. T. Chen, A. Y. Zhu, and F. Capasso, Nat. Rev. Mater. **5**, 604 (2020).
[2]R. Won, Nat. Photonics **13**, 585 (2019).
[3]A. M. Shaltout, K. G. Lagoudakis, J. van de Groep, S. J. Kim, J. Vučković, V. M. Shalaev, and M. L. Brongersma, Science **365**, 374 (2019).
[4]A. M. Shaltout, V. M. Shalaev, and M. L. Brongersma, Science **364**, eaat3100 (2019).
[5]J. Rho, MRS Bull. **45**, 180–187 (2020).
[6]N. Yu, P. Genevet, M. A. Kats, F. Aieta, J.-P. Tetienne, F. Capasso, and Z. Gaburro, Science **334**, 333 (2011).
[7]N. Yu and F. Capasso, Nat. Mater. **13**, 139 (2014).
[8]V. Ginis, M. Piccardo, M. Tamagnone, J. Lu, M. Qiu, S. Kheifets, and F. Capasso, Science **369**, 436 (2020).
[9]M. Y. Shalaginov, S. D. Campbell, S. An, Y. Zhang, C. Ros, E. B. Whiting, Y. Wu, L. Kang, B. Zheng, C. Fowler, H. Zhang, D. H. Werner, J. Hu, and T. Gu, Nanophotonics **9**, 3505 (2020).
[10]D. Maccaferri, I. Zubritskaya, I. Razdolski, I.-A. Chioar, V. Belotelov, V. Kapaklis, P. M. Oppeneer, and A. Dmitriev, J. Appl. Phys. **127**, 080903 (2020).
[11]A. Zvezdin and V. Kotov, *Modern Magnetooptics and Magnetooptical Materials*, Condensed Matter Physics (CRC Press, 2020).
[12]J. L. Costa-Krmer, C. Guerrero, S. Melle, P. Garcia-Mochales, and F. Briones, Nanotechnology **14**, 239 (2003).
[13]A. Syouji and H. Tominaga, J. Magn. Magn. Mater. **347**, 47 (2013).
[14]S. Mito, Y. Yoshihara, H. Takagi, and M. Inoue, AIP Adv. **8**, 056439 (2018).
[15]R. Higashida, N. Funabashi, K.-I. Aoshima, M. Miura, and K. Machida, Opt. Eng. **59**, 064104 (2020).
[16]T. R. Johansen, D. I. Norman, and E. J. Torok, J. Appl. Phys. **42**, 1715 (1971).
[17]D. Lacklison, G. Scott, H. Ralph, and J. Page, IEEE Trans. Magn. **9**, 457 (1973).
[18]G. Scott and D. Lacklison, IEEE Trans. Magn. **12**, 292 (1976).
[19]G. F. Sauter, M. M. Hanson, and D. L. Fleming, Appl. Phys. Lett. **30**, 11 (1977).
[20]J. A. Krawczak and E. J. Torok, IEEE Trans. Magn. **16**, 1200 (1980).
[21]T. Numata, Y. Ohbuchi, and Y. Sakurai, IEEE Trans. Magn. **16**, 1197 (1980).
[22]G. F. Sauter, R. W. Honebrink, and J. A. Krawczak, Appl. Opt. **20**, 3566 (1981).
[23]P. Hansen and J. P. Krumme, Thin Solid Films **114**, 69 (1984).
[24]D. Chen, J. F. Ready, and E. Bernal G, J. Appl. Phys. **39**, 3916 (1968).
[25]R. S. Mezrich, Appl. Phys. Lett. **14**, 132 (1969).
[26]H. Rll and K. Kempter, Opt. Commun. **16**, 83 (1976).
[27]G. Fan, K. Pennington, and J. H. Greiner, J. Appl. Phys. **40**, 974 (1969).
[28]T. Schmitte, A. Westphalen, K. Theis-Bröhl, and H. Zabel, Superlattices Microstruct. **34**, 127 (2003).
[29]M. Grimsditch and P. Vavassori, J. Phys. **16**, R275 (2004).
[30]P. Vavassori, N. Zaluzec, V. Metlushko, V. Novosad, B. Ilic, and M. Grimsditch, Phys. Rev. B **69**, 214404 (2004).
[31]U. B. Arnalds, E. T. Papaioannou, T. P. Hase, H. Raanaei, G. Andersson, T. R. Charlton, S. Langridge, and B. Hjörvarsson, Phys. Rev. B **82**, 144434 (2010).
[32]R. F. Wang, C. Nisoli, R. S. Freitas, J. Li, W. Mcconville, B. J. Cooley, M. S. Lund, N. Samarth, C. Leighton, V. H. Crespi, and P. Schiffer, Nature **439**, 303 (2006).
[33]Y. Perrin, B. Canals, and N. Rougemaille, Nature **540**, 410 (2016).
[34]C. Nisoli, V. Kapaklis, and P. Schiffer, Nat. Phys. **13**, 200 (2017).
[35]E. Östman, H. Stopfel, I.-A. Chioar, U. B. Arnalds, A. Stein, V. Kapaklis, and B. Hjörvarsson, Nat. Phys. **14**, 375 (2018).
[36]N. Rougemaille and B. Canals, Eur. Phys. J. B **92**, 62 (2019).
[37]S. H. Skjærvø, C. H. Marrows, R. L. Stamps, and L. J. Heyderman, Nat. Rev. Phys. **2**, 13 (2020).
[38]M. Agrawal, A. A. Serga, V. Lauer, E. T. Papaioannou, B. Hillebrands, and V. I. Vasyuchka, Appl. Phys. Lett. **105**, 092404 (2014).
[39]G. Schmidt, C. Hauser, P. Trempler, M. Paleschke, and E. T. Papaioannou, Phys. Status Solidi B **257**, 1900644 (2020).
[40]R. Bručas, H. Hafermann, I. L. Soroka, D. Iuşan, B. Sanyal, M. I. Katsnelson, O. Eriksson, and B. Hjörvarsson, Phys. Rev. B **78**, 024421 (2008).
[41]H. Haskal, IEEE Trans. Magn. **6**, 542 (1970).
[42]M. Tanaka, T. Ito, and Y. Nishimura, IEEE Trans. Magn. **8**, 523 (1972).
[43]R. M. Rowan-Robinson, J. Hurst, A. Ciuciulkaite, I.-A. Chioar, M. Pohlit, M. Zapata-Herrera, P. Vavassori, A. Dmitriev, P. M. Oppeneer, and V. Kapaklis, Adv. Photonics Res. **2**, 2100119 (2021).
[44]K. Mishra, A. Ciuciulkaite, M. Zapata-Herrera, P. Vavassori, V. Kapaklis, T. Rasing, A. Dmitriev, A. Kimel, and A. Kirilyuk, Nanoscale **13**, 19367 (2021).
[45]S. Mangin, M. Gottwald, C.-H. Lambert, D. Steil, V. Uhlíř, L. Pang, M. Hehn, S. Alebrand, M. Cinchetti, G. Malinowski, Y. Fainman, M. Aeschlimann, and E. E. Fullerton, Nat. Mater. **13**, 286 (2014).
[46]A. Ciuciulkaite, K. Mishra, M. V. Moro, I.-A. Chioar, R. M. Rowan-Robinson, S. Parchenko, A. Kleibert, B. Lindgren, G. Andersson, C. S. Davies, A. Kimel, M. Berritta, P. M. Oppeneer, A. Kirilyuk, and V. Kapaklis, Phys. Rev. Mater. **4**, 104418 (2020).
[47]D. Ksenzov, A. A. Maznev, V. Unikandanunni, F. Bencivenga, F. Capotondi, A. Caretta, L. Foglia, M. Malvestuto, C. Masciovecchio, R. Mincigrucci, K. A. Nelson, M. Pancaldi, E. Pedersoli, L. Randolph, H. Rahmann, S. Urazhdin, S. Bonetti, and C. Gutt, Nano Lett. **21**, 2905–2911 (2021).
[48]B. Wang, K. Rong, E. Maguid, V. Kleiner, and E. Hasman, Nat. Nanotechnol. **15**, 450 (2020).
[49]R. A. Beth, Phys. Rev. **48**, 471 (1935).
[50]R. A. Beth, Phys. Rev. **50**, 115 (1936).
[51]L. Allen, M. W. Beijersbergen, R. J. C. Spreeuw, and J. P. Woerdman, Phys. Rev. A **45**, 8185 (1992).
[52]J. S. Woods, X. M. Chen, R. V. Chopdekar, B. Farmer, C. Mazzoli, R. Koch, A. S. Tremsin, W. Hu, A. Scholl, S. Kevan, S. Wilkins, W.-K. Kwok, L. E. De Long, S. Roy, and J. T. Hastings, Phys. Rev. Lett. **126**, 117201 (2021).